⊕ISME

ARTICLE

Functional genome-centric view of the CO-driven anaerobic microbiome

Haowen Duan[1] · Pinjing He[2] · Liming Shao[2] · Fan Lü ◉[1,3]

Abstract
CO is a promising substrate for producing biochemicals and biofuels through mixed microbial cultures, where carboxydotrophs play a crucial role. The previous investigations of mixed microbial cultures focused primarily on overall community structures, but under-characterized taxa and intricate microbial interactions have not yet been precisely explicated. Here, we undertook DNA-SIP based metagenomics to profile the anaerobic CO-driven microbiomes under 95 and 35% CO atmospheres. The time-series analysis of the isotope-labeled amplicon sequencing revealed the essential roles of Firmicutes and Proteobacteria under high and low CO pressure, respectively, and *Methanobacterium* was the predominant archaeal genus. The functional enrichment analysis based on the isotope-labeled metagenomes suggested that the microbial cultures under high CO pressure had greater potential in expressing carboxylate metabolism and citrate cycle pathway. The genome-centric metagenomics reconstructed 24 discovered and 24 under-characterized metagenome-assembled genomes (MAGs), covering more than 94% of the metagenomic reads. The metabolic reconstruction of the MAGs described their potential functions in the CO-driven microbiomes. Some under-characterized taxa might be versatile in multiple processes; for example, under-characterized *Rhodoplanes* sp. and *Desulfitobacterium_A* sp. could encode the complete enzymes in CO oxidation and carboxylate production, improving functional redundancy. Finally, we proposed the putative microbial interactions in the conversion of CO to carboxylates and methane.

Introduction

Most CO-utilizing microbes are facultative lithotrophs that are capable of using organic substrates as carbon and energy sources [1–5]; therefore, the term carboxydotroph used here and in other studies defines all the microbes capable of using CO as energy source through carbon monoxide dehydrogenase (CODH) [4–6]. As per cofacter contents,

CODHs can be classified into aerobic (Mo-containing) and anaerobic (Ni-containing) types. CODHs are present in physiologically and phylogenetically diverse bacteria and archaea [2, 7], in which CO oxidation can be coupled to oxygen respiration, proton respiration, sulfate respiration, acetogenesis, and methanogenesis [8]. Carboxydotrophs play essential roles in global carbon flux such as holding the concentration of atmospheric CO below toxic level [9–12], and carboxydotrophs are of potential biotechnological interest for synthesis gas (syngas) fermentation as a biorefinery factory [13, 14]. For both fossil-based waste and biogenic but biologically recalcitrantly degradable waste, coupling syngas production to biorefinery is a promising approach to produce value-added biochemicals and to improve bioenergy recovery from waste [15–17]. Additionally, this combined process can overcome the inherent limitations of chemical catalyzers in syngas conversion [18, 19]. CO is a main component of syngas, and the potential of CO/CO_2 couple ($E^{0\prime} = -520$ mV) theoretically is more favorable for higher energy conservation than hydrogen oxidation ($E^{0\prime} = -414$ mV) [20]. Unfortunately, despite the low reduction potential of CO, the microbial

✉ Fan Lü
lvfan.rhodea@tongji.edu.cn

1 State Key Laboratory of Pollution Control and Resource Reuse, Tongji University, Shanghai, China

2 Institute of Waste Treatment and Reclamation, Tongji University, Shanghai, China

3 Shanghai Institute of Pollution Control and Ecological Security, Shanghai, China

tolerance and utilization for CO is a bottleneck for CO bio-utilization. Thus, insights into carboxydotrophs and their interactions with other microbes will yield useful information about CO bioconversion processes.

Previous studies about the carboxydotrophs in CO bioconversion were primarily concerned with model or isolated microbes in pure culture [21, 22]. Briefly, mesophilic carboxydotrophs can exploit CO to predominantly form chemicals such as carboxylates and alcohols [23, 24]. And various studies have determined the physiological characteristics of carboxydotrophic acetogens; for example, *Clostridium ljungdahlii* is a well-studied model to produce acetate and ethanol through Wood–Ljungdahl pathway [13]. Methanogens are the best-studied carboxydotrophic archaea [4]. Four methanogens have been demonstrated to grow on CO as a sole substrate [20], and acetate formation was observed during the carboxydotrophic growth of *Methanosarcina acetivorans* C2A and *Methanothermobacter marburgensis* [21, 25]. However, there is still a tremendous number of under-characterized taxa with carboxydotrophic potential in artificial and natural environments [26–28]. For instance, few mesophilic carboxydotrophs perform thermodynamically favorable H_2 production, where CO is firstly oxidized by CODH and the derived electrons are used to reduce protons via an energy-converting hydrogenase [29, 30]. Moreover, the anaerobic CO oxidation in Proteobacteria has not been further investigated [30]. These indicate that carboxydotrophs may be phylogenetically more diverse than expected, and a requirement arises for broadening the phylogenetic scope of carboxydotrophs. Until now, most studies about mixed microbial cultures mainly explored the effects of environmental factors on product spectrum and overall microbial community structures using 16S rRNA gene sequencing [31–34]. Few studies explicitly explored the under-characterized taxa and the genome-centric interactions in the mixed microbial cultures fed with CO, as well as the functional potential in these cultures. Therefore, the genome reconstruction and annotation of microbes, e.g., the non-carboxydotrophs which utilize the CO-derived metabolites of carboxydotrophs (that is, CO_2, acetate and others), is necessary to uncover the black-box microbial ecology of a CO-driven microbiome.

Metagenomics can profile the functional potential of microbial communities and reconstruct the genomes of under-characterized taxa [35]. Despite its success, some limitations to this technique also exist. Metagenomic sequencing of bulk DNA extracted directly from environmental samples may overlook the potentially essential roles of rare species [36]. The increased complexity of microbial communities dramatically hinders metagenomic assembly, leading to the limited reconstruction of high-quality genomes [37, 38]. Furthermore, metagenomics does not allow to confirm the potential functions of under-characterized microbes. However, stable isotope probing (SIP) can help to

confirm the connection between functions and microbes [39, 40], and DNA-SIP has an enormous advantage in enriching the DNA of functional microbes through a physical filtering to improve metagenomic assembly [41]. DNA-SIP based metagenomics has been applied to environmental samples [42–45]; thus, this method should be feasible to explore CO-driven microbiomes.

To address the above knowledge gaps, DNA-SIP based metagenomics was applied in this work to explore the CO-driven microbiomes under different initial CO pressures. The dynamic succession of functional microbiotas was described through the time-series analysis of the labeled 16S rRNA genes. Functional enrichment analysis unraveled the enriched functional potential of the microbiomes under high CO pressure. Additionally, genome-centric analysis reconstructed the metagenome-assembled genomes (MAGs) of under-characterized taxa. Based on the metabolic reconstruction of the MAGs, the ecological role of each species in the conversion of CO to end-products was identified, and the putative microbial interactions in the mixed microbial cultures were established. This in-depth and precise characterization of the CO-driven microbiomes is expected to contribute in the understanding of biodiversities and interactions within mixed microbial cultures, as well as the operating conditions of CO bio-utilization.

Materials and methods

Methods are described in detail in the Supplementary Methods.

Anaerobic incubation with ^{13}CO

Inoculum that had acclimatized to a CO atmosphere of 0.6 atm was sampled from a mesophilic batch reactor at 35 °C with pH ranging from 6.8 to 7.1. Microcosms were set up by using 570 ml serum bottles filled with 150 ml basal medium as in our previous study [46], and the initial pH was adjusted to 7.0. The inoculum was seeded at a concentration of 1 g/l volatile solid to enhance isotope labelling. Each bottle was sealed with a screw cap and a rubber septum, and the headspace was vacuumized and purged with high purity N_2 (99.999%) three times before injecting CO. Two experiments were carried out and denoted as "high P_{CO}" and "low P_{CO}", where the initial CO pressures were 0.95 and 0.35 atm, respectively. For each CO pressure, there were two groups of microcosms. The first group of triplicate microcosms contained ^{13}CO (99 atom% in ^{13}C, Cambridge Isotope Laboratory, USA). The second group of triplicate microcosms was fed with ^{12}CO. The total pressure in each microcosm was 1 atm using complementary N_2. All microcosms were maintained at 35 °C and pH

6.0–7.0 using 1 M HCl or 1 M NaOH solution, and were stirred at 125 rpm in a shaker. The negative pressure in serum bottles owing to CO consumption was adjusted to 1 atm by injecting high purity N_2 (99.999%). Every 4 days, the headspace of each microcosm was vacuumized and readjusted to the initial CO pressures. Gas pressure, gas composition, pH, and carboxylate (C_2–C_7, referring to total dissociated and undissociated carboxylic acid) concentration before and after vacuuming were measured, and the incorporation of ^{13}C and ^{12}C into carboxylates was monitored.

DNA extraction, isopycnic centrifugation, and fractionation

Sludge fed with ^{12}CO and ^{13}CO was collected for DNA extraction after 12, 24, and 36 days of incubation (labeled the 12th, 24th, and 36th days, respectively). DNA was extracted and subjected to isopycnic centrifugation and fractionation. CsCl density gradient ultracentrifugation was performed at 51,800 rpm (about $194,991 \times g$) and 20 °C for 40 h in biological and technological triplicate. After centrifugation, 24 gradient fractions of 200 μl were recovered, and the buoyant density and DNA concentration of each fraction were measured. Most DNA from the sludge fed with ^{12}CO was detected at buoyant densities of 1.68–1.72 g/ml, and the DNA concentration was under detection limit at densities higher than 1.72 g/ml. The DNA from ^{13}C-fed sludge showed an increase in densities of 1.73–1.76 g/ml, regardless of CO pressure (Fig. S1). Therefore, in the sludge fed with ^{13}CO, the fractions with densities of 1.73–1.76 g/ml and the remaining fractions with densities <1.73 g/ml were pooled and designated "heavy fractions" and "light fractions", respectively. The fractions with densities of about 1.68–1.72 g/ml were designated "control fractions" when ^{12}CO was fed as substrate.

Amplicon sequencing and analysis

The DNA in the heavy, light, and control fractions from the triplicate samples of each condition was used for amplicon sequencing, where the samples at three incubation time were considered (Dataset S1). Amplification of V4 region was carried out using primer F515 (5′-GTGCCAGCMGCCGCGG-TAA-3′) and R806 (5′-GGACTACVSGGGTATCTAAT-3′) [47]. Briefly, the PCR program was performed: 95 °C for 3 min, then 27 cycles of 95 °C for 30 s, 55 °C for 30 s, and 72 °C for 45 s. A final extension at 72 °C was kept for 10 min and the products were held at 4 °C. The purified PCR products were pooled in equimolar and paired-end sequenced (2 × 300 bp) on a MiSeq platform (Illumina, San Diego, USA). Raw amplicon reads were denoised and dereplicated into amplicon sequence variants (ASVs) using DADA2 v.1.10 [48]

before clustering into 97% operational taxonomic units (OTUs) with VSEARCH v.2.7.0 [49]. Taxonomic classification of each ASV or OTU was performed using the VSEARCH-based classifier in QIIME 2 v.2019.4 [50] against the SILVA 16S rRNA gene database (132 release). Diversity measurements were carried out using Vegan v.2.5-3 [51]. Microbial networks were constructed using the OTUs in the heavy fractions under high CO and low CO pressure through MENAP [52], respectively.

Metagenomic sequencing and analysis

The DNA in the heavy fractions of the triplicate samples for the same condition was used for metagenomic sequencing, where the samples were collected at the 12th and 24th days. Briefly, sequencing libraries were prepared using NEB-Next® UltraTM DNA Library Prep Kit for Illumina (New England Biolabs, USA). The libraries were analyzed for fragment size distribution by Agilent2100 Bioanalyzer (Agilent Technologies) and were paired-end sequenced (2 × 150 bp) on Illumina platforms according to the standard protocols. Raw metagenomic reads were trimmed with fastp v.0.20.0 to obtain clean reads [53], which were then corrected and assembled into 12 single assemblies and four co-assemblies using metaSPAdes v.3.13.1 (Table S1) [54]. For each assembly, three bin sets were generated using Max-Bin2 v.2.2.6 [55], MetaBat2 v.2.12.1 [56], and CONCOCT v.1.1.0 [57]. All the bins in the three bin sets were checked using CheckM v.1.0.13 [58]. All bins of the 16 assemblies were dereplicated to produce MAGs using dRep v.2.6.2 (Table S1) [59]. The abundances of the MAGs were quantified across 12 samples using metaWRAP v.1.2 [60]. Genome Taxonomy Database(GTDB)-Tk v.1.3.0 was used to identify the taxonomic classifications of the MAGs based on the GTDB (05-RS95 release) [61, 62]. The terms discovered and under-characterized defined the MAGs with and without published genomes, respectively. The coding sequences of the MAGs were predicted and annotated using Prodigal v.2.6.3 and eggNOG-mapper v.2.0.1, respectively [63, 64]. In functional enrichment analysis, the genes were annotated and quantified across 12 samples using HUMAnN2 v.2.8.2 [65]. Then, the genes were clustered into functional categories based on the KEGG Orthogroups (KOs). The principal coordinates analysis using the relative abundances of the KOs showed that the 1st biological triplicate under low CO pressure were outliers (Fig. S2); therefore, for increasing sensitivity, only the 2nd and 3rd biological triplicate under low CO pressure were used to make the differential comparison in the relative abundances of a specific KO between high CO and low CO pressure at the same incubation time. The KOs with significantly differential abundances ($p < 0.05$, Welch's t test) between high CO and low CO pressure were used to perform functional
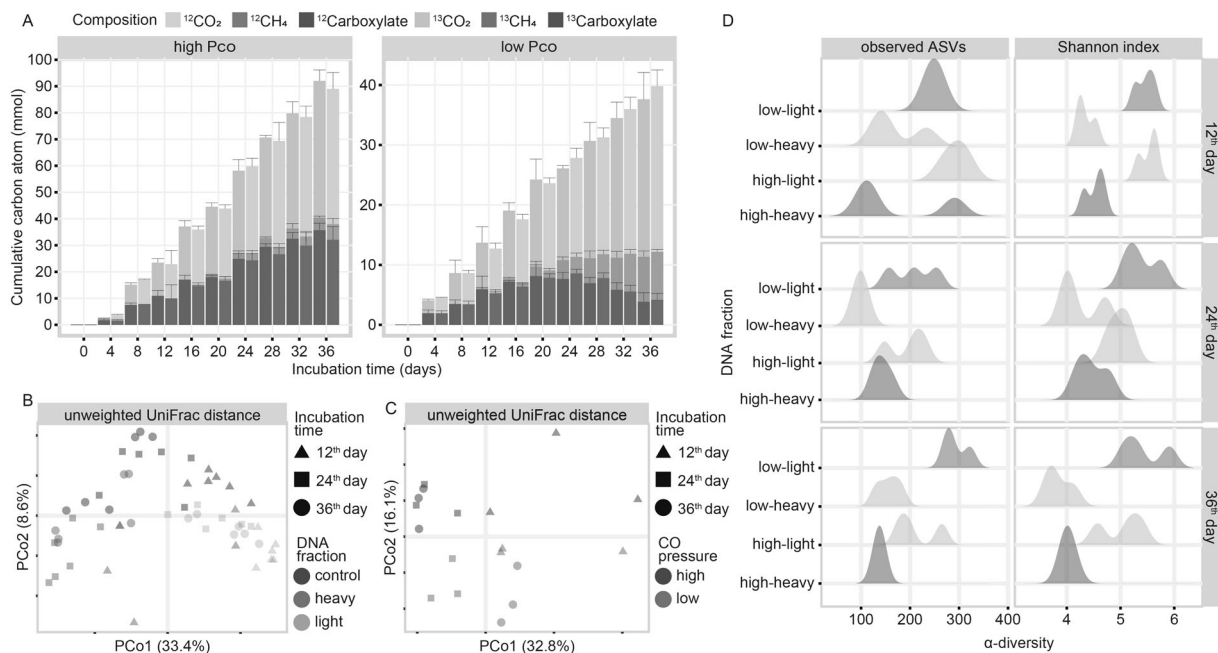
Fig. 1 The properties of the microbiotas between different CO pressures or incubation time. A Cumulative carbon atom quantities of the carbonaceous compositions in the microcosms. The blue bars and its left red bars indicated the carbonaceous compositions in the microcosms fed with ^{12}CO and ^{13}CO at the same incubation time, respectively. The value of each bar represented an average value of biological triplicate ($n = 3$), and the error bars donated the standard deviation. The error bars of methane were shown when its cumulative carbon atom quantities were more than 0.1 mmol. **B** The β-diversity measurement using unweighted UniFrac distance (UUD). All the heavy fractions, light fractions, and control fractions under high CO and low CO pressure were considered. **C** The β-diversity measurement using unweighted UniFrac distance (UUD). Only the heavy fractions under high CO and low CO pressure were considered. **D** The α-diversity measurements in all the heavy fractions and light fractions using the number of the observed individuals and Shannon index based on ASVs. The densities were calculated from the point data mapped onto the x-axis ($n = 3$), and the higher ridges, the more concentrated the values of biological triplicate were (Color figure online).

enrichment analysis based on the KEGG pathway and module.

Results and discussion

Conversion of CO under different CO pressures

There was no significant difference in the cumulative carbon atom quantity of each carbonaceous composition between the microcosms fed with ^{13}CO and ^{12}CO, regardless of CO pressure ($p > 0.05$, Wilcoxon test; Fig. 1A and Table S2). This result indicated that when compared with the microcosms fed with ^{12}CO, the addition of ^{13}CO did not affect the microbial utilization of CO or the microbial community structures. Therefore, ^{13}CO just labeled the microbes that participated in the utilization of CO or CO-derived metabolites, and the above confirmation of the fractions based on buoyant densities was reliable. Approximately 98 and 41 mmol CO were totally consumed under high CO and low CO pressure, respectively. More than 90 C-atom% of the consumed CO was converted to carboxylates, CH_4 and CO_2 throughout the experiments

(Fig. S3), where CO_2 accounted for more than 50 C-atom% regardless of CO pressure, indicating the active enzymatic reaction of CODH. The conversion ratio of CO to CH_4 exceeded 1 C-atom% on the 20th day under high CO pressure, and the ratio increased up to ~5 C-atom%. However, CH_4 accounted for more than 1 C-atom% of the consumed CO under low CO pressure from the 12th day, and the ratio rapidly increased up to 16 C-atom% (Fig. S3). These results agreed well with the view that methanogens are less resistant to high CO pressure [26, 66]. Under low CO pressure, acetate, propionate, and butyrate contributed to most of the carboxylates, and almost all kinds of the carboxylates began to decrease from the 24th day on (Figs. S4 and S5), indicating that other microbes might be involved in the degradation of carboxylates in addition to methanogens, which cannot use substrates such as butyrate. Approximately 35 C-atom% of the consumed CO was concentrated in carboxylates under high CO pressure (Fig. S3), and the ratio of acetate was less than that under low CO pressure (Fig. S4); therefore, more carbon flowed into longer carbon chain carboxylates, such as butyrate and heptylate. These results showed that high CO pressure might be conducive to the synthesis of longer carbon chain

carboxylates, which reduced the carbon flow into CH_4. In the microcosms fed with ^{13}CO, the median ratios of fully ^{13}C-labeled carboxylate fragments were almost all above 90% (Fig. S6), indicating the active uptake and turnover of the added ^{13}CO. Previous studies on mixed microbial cultures showed that acetate was a predominant carboxylate, and CH_4 was only produced under low CO pressure [6, 26, 31, 67, 68]. Butyrate might be the carboxylate with the longest carbon chain in the previous studies. Although a previous study achieved longer carbon chain carboxylate production, 2-bro-moethanesulfonate was added to inhibit methanogenesis [69]. Valerate, caproate, and heptylate were produced in the present work, suggesting the active carbon chain elongation in the microbial cultures and demonstrating the feasibility of medium-chain carboxylate production without adding methanogenesis inhibitors. Additionally, increased CO tolerance threshold of methanogenesis in this study might be due to the methanogens' adaptation to CO after a long-term exposure.

Core microbes under different ^{13}CO pressures

Amplicon sequencing of the 16S rRNA genes was performed to determine the composition and diversity of each microbiota. An average read count per sample of 48,855 was obtained, which covered the majority of the microbiotas (Dataset S1 and Fig. S7). All microbiotas in the principle coordinates analysis (PCoA) using unweighted UniFrac distance (UUD) could be grouped significantly by the fractions, as could the PCoAs using other distances (Figs. 1B and S8, $p = 0.001$, Dataset S2). Partial canonical analysis of principal coordinates also revealed the significant effect of the fractions on the microbiotas (Fig. S9, $p = 0.001$). These findings suggested that isotope labeling isolated the core microbes and cross-feeding was minor. CO pressure significantly contributed to the differences in the microbiotas and explained 14.4%, 25.4%, 15.7%, and 26.3% of the variation when using UUD, Bray–Curtis (BCD), Jaccard (JCD), and weighted UniFrac (WUD) distances, respectively (Figs. 1C and S10, $p < 0.05$, Dataset S3 and Dataset S4). BCD and WUD take the microbial abundances into consideration, whereas JCD and UUD do not; thus, the higher explanation ratios of CO pressure using BCD and WUD indicated that CO pressure might cause relatively large shifts in microbial abundances. Another factor significantly shaping the microbiotas was incubation time (Figs. 1C and S10A, B, $p < 0.05$, Dataset S3 and Dataset S4). Furthermore, the interaction between CO pressure and incubation time significantly comprised 14.0% and 16.9% of the variation based on BCD and WUD, respectively ($p < 0.05$, Dataset S4), but this interaction had no significant impact on the variation based on JCD and UUD ($p > 0.05$, Dataset S4), highlighting the changes in the microbial abundances.

The α-diversity was measured using the number of observed individuals and Shannon index, considering the richness and evenness of microbiotas. The median α-diversity was significantly higher in the light fractions than that in the heavy fractions under the same CO pressure or incubation time (Fig. 1D, $p < 0.05$, Dataset S5). This finding showed that the number of the species which participated in the conversion of CO or CO-derived metabolites might not occupy the majority of the total number of species in the microbiotas, and suggested the existence of the predominant microbes with high abundances in the heavy fractions, resulting in the lower evenness. The observations based on OTUs agreed well with the above results (Dataset S5). The mean α-diversity in the heavy fractions based on ASVs was significantly higher than that based on OTUs ($p < 0.001$, Wilcoxon test), but the mean α-diversity in the light fractions based on ASVs was similar with that based on OTUs (Fig. S11). This result suggested that the microbiotas in the heavy fractions had higher microdiversity, where one OTU might contain multiple functionally equivalent ASVs, that is, several species consisted of many different subpopulations. Microdiversity is essential for microbial community stability [70], and recent studies have demonstrated that different subpopulations of the same species sustain the distribution of this species across broad environmental gradients [71, 72]. Therefore, the microbes in the heavy fractions might be more resistant to variable CO pressure than those in the light fractions.

Proteobacteria and Firmicutes were significantly enriched in the heavy fractions at the 12th day, regardless of CO pressure (Fig. S12). As the incubation time progressed, the abundance of Proteobacteria showed a significant decrease in the heavy fractions under high CO pressure. However, under low CO pressure, Proteobacteria was always significantly enriched in the heavy fractions where its abundance remained stable (Fig. 2A). The predominant genus in Proteobacteria was *Rhodoplanes*, which was almost all significantly enriched in the heavy fractions under low CO pressure (Figs. 2B and S13). Complete CODH genes have been found in the isolated *Rhodoplanes* sp. Z2-YC6860, but the CO metabolism of *Rhodoplanes* has not been previously investigated in the literature. Under high CO pressure, Firmicutes was always significantly enriched in the heavy fractions where its abundance showed a significant increase, but under low CO pressure, a significant drop in its abundance was noted throughout the incubation (Figs. 2A and S12). Although *Clostridium* is known for carboxylate synthesis, the prevalent genus of Firmicutes in this work was *Acetobacterium* (Fig. 2B), of which some species are carboxydotrophic acetogens [22, 23, 73]. Under high CO pressure, *Acetobacterium* was significantly enriched in the heavy fractions where the abundance of *Acetobacterium* showed a significant increase (Fig. S13), suggesting that it
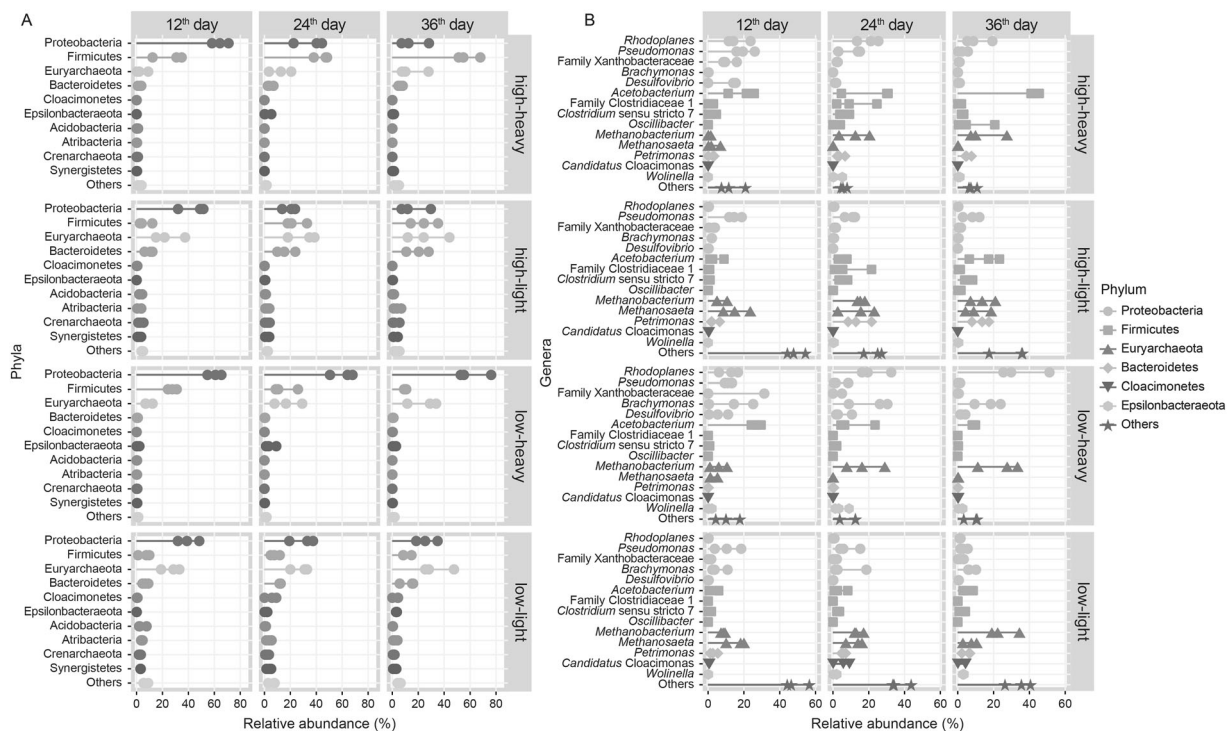
Fig. 2 The dynamic succession of predominant taxa. A phylum level. **B** genus level. The phylum and genus with a maximum relative abundance greater than 9% and 5% were selected, respectively. The label "Others" represented the total relative abundance of remining taxa. The three dots of each taxon represented biological triplicate ($n = 3$). The labels "High" and "Low" indicated CO pressures, and the labels "heavy" and "light" indicated fractions.

was a keystone taxon in acetate production. Additionally, *Oscillibacter* was only detected under high CO pressure (Fig. 2B), which has received limited attention in CO utilization. Methanogenesis was an essential metabolic process in this work and was performed by the methanogens of Euryarchaeota, which was found to be mainly composed of *Methanobacterium* and *Methanosaeta* (Fig. 2B). Some previous mesophilic studies showed that acetoclastic methanogenesis was dominant when CO pressure was below 0.5 atm [34, 74], where acetoclastic methanogens should be abundant. However, the present work disclosed that *Methanobacterium* was the predominant archaeal genus, regardless of CO pressure. The increased abundance of *Methanobacterium* under both CO pressures implied its wide tolerance range to CO. Despite the high acetate concentration, the acetoclastic methanogen *Methanosaeta* was almost all significantly enriched in the light fractions (Fig. S13), indicating that cross-feeding might be minor. The truncated power laws of the co-occurrence networks under high CO and low CO pressure were both fitted well (Table S3), and these networks displayed small-world characteristics (Table S4 and Supplementary Notes). The networks also showed the predominant roles of Proteobacteria, Firmicutes, and Euryarchaeota, which totally occupied ~64% and 47% of the nodes under high CO and low CO pressure, respectively (Dataset S6).

Functional potential of the microbiomes under high CO pressure

As far as we know, no previous research has investigated the effects of high CO pressure on functional potential; therefore, the significantly differential KOs between two CO pressures were used to perform functional enrichment analyses (Dataset S7). Overall, 43 and 18 pathways had significantly greater potential under high CO pressure than under low CO pressure at the 12th and the 24th days, respectively (Fig. 3 and Dataset S8). At the 12th day, the pathways relating to fatty acids were significantly enriched under high CO pressure, including carbon fixation in prokaryotes, butanoate metabolism, propanoate metabolism, and fatty acid biosynthesis. Some enzymes of these pathways can participate in Wood–Ljungdahl pathway and reverse β-oxidation (RBO), which are essential for synthesizing acetate and longer carbon chain carboxylates, respectively. These results suggested that the microbiomes under high CO pressure had greater potential in carboxylate production, resulting in the accumulation of carboxylates with 3–7 carbons under high CO pressure. At the 12th and 24th days, the potential in citrate cycle (TCA cycle) was significantly greater under high CO pressure than under low CO pressure. In anaerobic microbes, TCA-related genes have potential in synthesizing essential biosynthetic
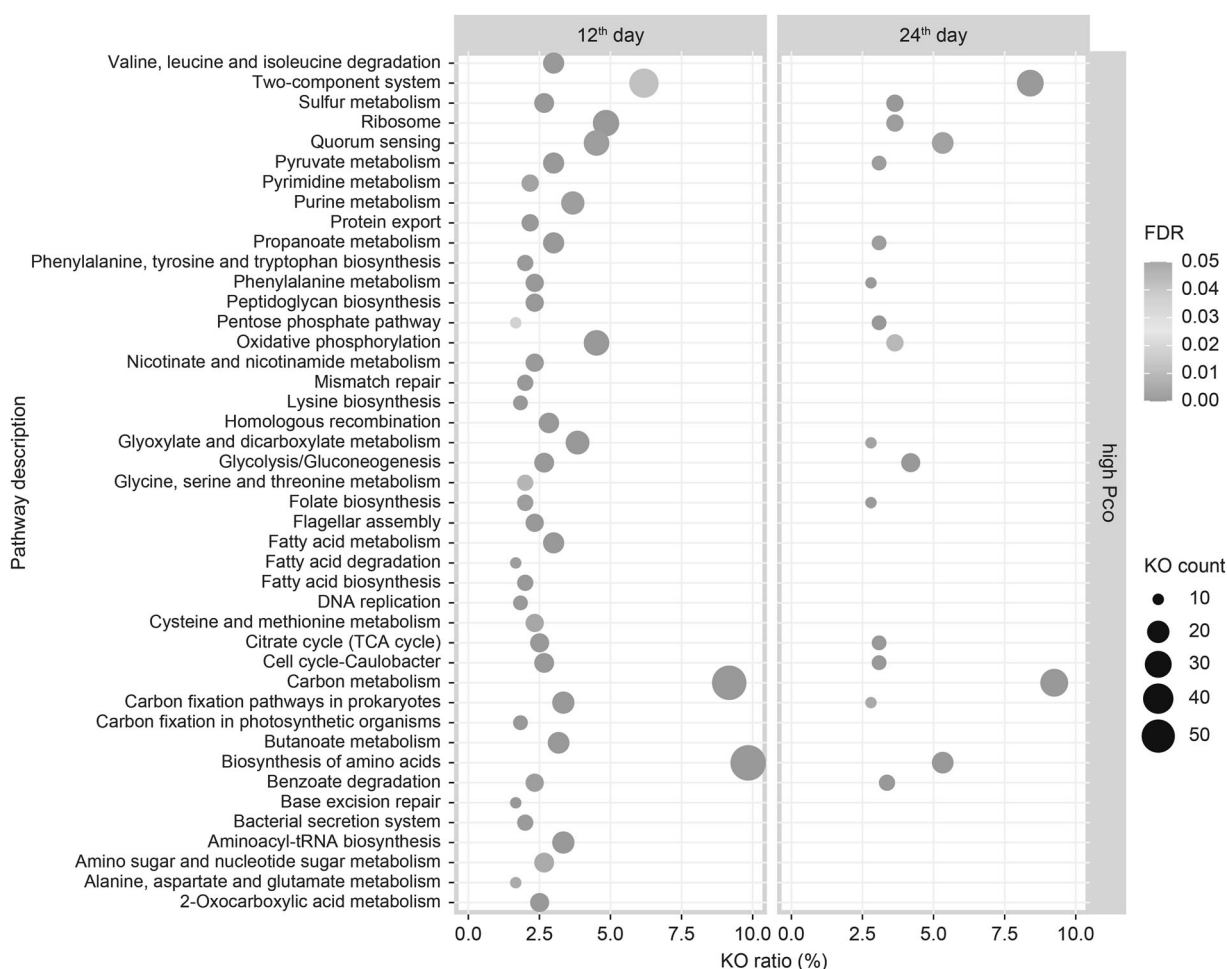
Fig. 3 The functional enrichment analyses using the significantly increased KOs under high CO pressure. Benjamini and Hochberg method was used to verify the statistical significance. The pathways with KO counts <10 were filtered. KO ratio was calculated by dividing k by n, where k (KO count) was the number of the significantly increased KOs in a specific KEGG pathway and n was the number of the significantly increased KOs in all KEGG pathways.

intermediates such as succinate and 2-oxoglutate [75]. These intermediates can be used in amino acid, pyrimidine, and purine metabolism, and the biosynthesis of amino acids was significantly enriched under high CO pressure. The functional enrichment analyses based on the KEGG module also showed that citrate cycle was significantly enriched under high CO pressure (Fig. S14). These results indicated that the microbes under high CO pressure might exhibit greater potential in maintaining fundamental metabolism than those under low CO pressure.

Microbial interactions revealed by genome-centric metagenomics

Twenty-eight MAGs from co-assembly and 20 MAGs from single assembly were reconstructed (completeness >70%, contamination <10%), spanning nine bacterial and three archaeal phyla (Fig. 4 and Dataset S9). More than 94% of the metagenomic reads could be mapped to these

MAGs; therefore, it was assumed that these MAGs provided a comprehensive representation of the CO-driven microbiomes. These MAGs were further categorized into six groups (group A–F) based on their functional characteristics.

CO oxidation

As the initial carbon source was CO, carboxydotrophs were essential to fix carbon and provide available carbon sources for other microbes. Carbon monoxide dehydrogenase/acetyl-CoA synthase (CODH/ACS) complex α subunit (*acsA*) and its homolog anaerobic CODH catalytic subunit (*cooS*) were used to identify anaerobic carboxydotrophs. In total, six under-characterized MAGs and six discovered MAGs made up group A, where CO oxidation might be performed (Figs. 5 and S15, Dataset S10 and Dataset S11). These carboxydotrophs played an essential role in reducing the inhibition level of CO. MAG H3 was identified as an
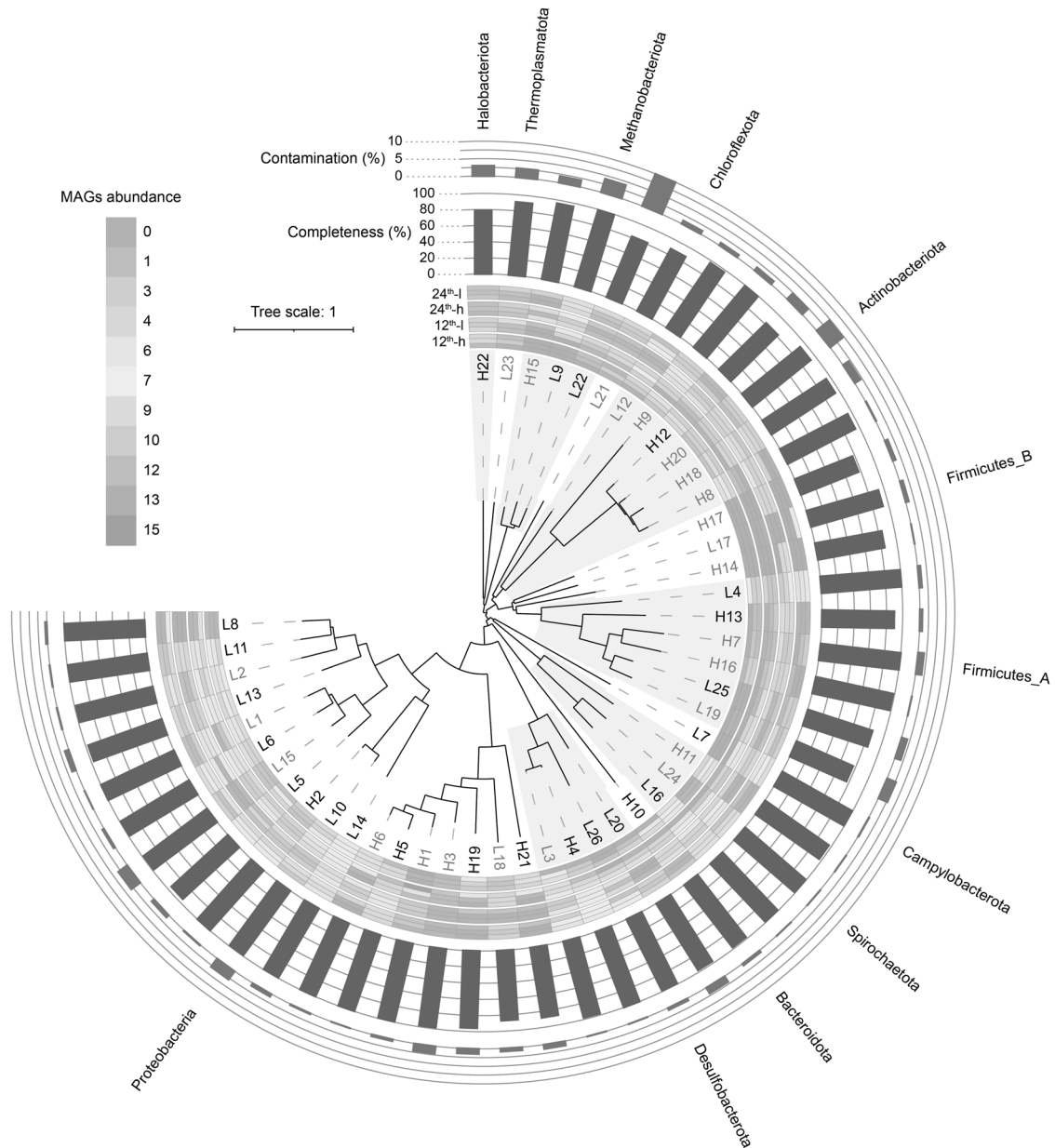
Fig. 4 The phylogenetic tree of the dereplicated MAGs reconstructed using all assemblies. The bacterial and archaeal MAGs with completeness >70% and contamination <10% were considered. For the label of MAG, "H" and "L" represented this MAG has a higher average abundance under high CO and low CO pressure, respectively. The black labels of the MAGs represented that these MAGs were assigned to discovered species or public genomes, and the red labels of the MAGs represented that these MAGs were under-characterized

species. The completeness and contamination of each MAG were shown in the blue and red barplot, respectively. The abundances of each MAG under two CO pressures were shown in the heatmap. The abundances were expressed as genome copies per million reads (CPM), which had been standardized to individual genome size, and these abundances were logarithmically processed as $Log_2(CPM + 1)$ for visualization (Color figure online).

under-characterized species of phototrophic *Rhodoplanes*, in which no carboxydotrophic growth is known [76]. The complete genes encoding CODH and CODH-induced hydrogenase, which are essential in carboxydotrophic proton respiration [29, 77], were found in *Rhodoplanes* H3. Additionally, these genes were highly similar in sequence content and gene organization with the well-characterized

homologs of *Rhodospirillum rubrum*, which is a model hydrogenogenic carboxydotroph (Fig. S16) [78, 79], suggesting that *Rhodoplanes* H3 could perform carboxydotrophic hydrogenesis. Few mesophiles have been identified as anaerobic hydrogenogenic carboxydotrophs, and these mesophiles are all phototrophic Proteobacteria [30, 76]. Nevertheless, the high relative abundances of Proteobacteria
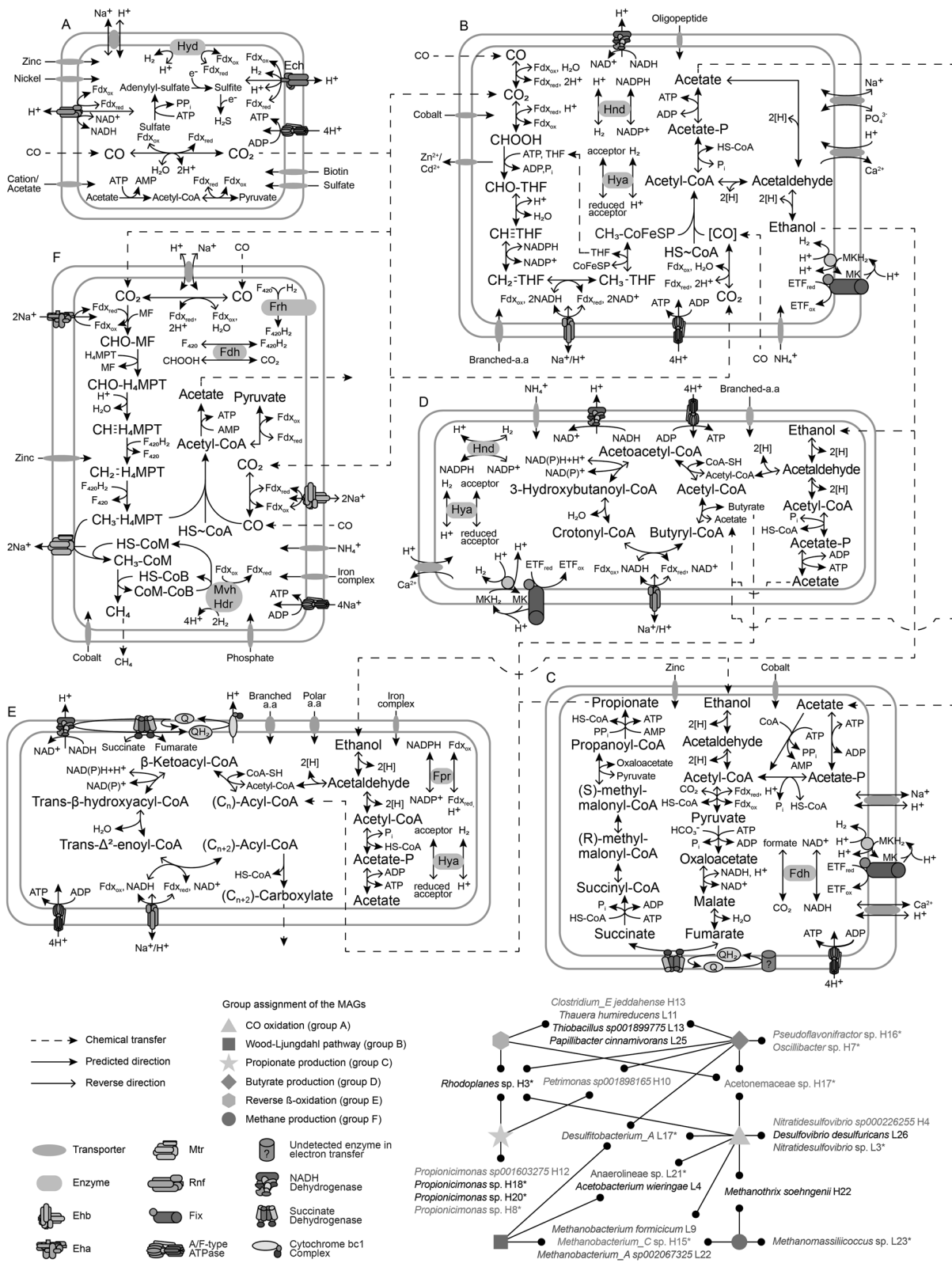
have been detected in some studies fed with CO [46, 80], indicating that anaerobic CO oxidation should be widespread in Proteobacteria. The emergence of *Rhodoplanes*

H3 expanded the phylogenetic diversity of mesophilic hydrogenogenic carboxydotrophs and proposed the crucial role of Proteobacteria in anaerobic CO oxidation [76].

Fig. 5 The representative metabolic pathways in each group, and the microbial interactions among groups. Only the metabolic pathways related to the main function of each group were shown. The under-characterized MAGs *Nitratidesulfovibrio* L3, *Desulfitobacterium_A* L17, *Propionicimonas* H18, *Oscillibacter* H7, Acetonemaceae H17, and *Methanobacterium_C* H15 were the representative genomes of groups A–F, respectively. The reverse direction of enzyme only indicated the potential of reversible enzymatic reaction. Asterisk indicated these MAGs were under-characterized taxa, and the other MAGs were assigned to discovered species or published genomes. The exact stoichiometries were not considered in this figure. Mtr tetra-hydromethanopterin S-methyltransferase, Rnf *Rhodobacter* nitrogen fixation complex, Eha energy-converting hydrogenase A, Ehb energy-converting hydrogenase B, Fix electron-transfer-flavoprotein (ETF)-oxidizing hydrogenase complex.

Carboxylate synthesis

Apart from CO_2, the primary metabolites were carboxylates (C_2–C_7, referring to total dissociated and undissociated carboxylic acid, Fig. 1A), which were mainly acetate (Fig. S4). Wood–Ljungdahl pathway is necessary for acetate production from CO or CO_2, and this pathway has four maker genes, acetyl-CoA synthase (*acsB*), corrinoid iron sulfur proteins (*acsC* and *acsD*), and formate-tetrahydrofolate ligase (*fhs*) [23, 81, 82]. Two under-characterized and a discovered bacterial MAGs could encode the complete maker genes and other genes in Wood–Ljungdahl pathway; therefore, they constituted group B, which provided acetate or ethanol for other microbes (Figs. 5 and S15, Dataset S10 and Dataset S11). The under-characterized MAGs L21 and L17 were assigned to a novel genus of class Anaerolineae and a novel species of genus *Desulfitobacterium_A*, respectively. Their emergence suggested that the high phylogenetic diversity of the microbes performing Wood–Ljungdahl pathway and further studies are needed to explore this function guild. *Desulfitobacterium_A* L17 might also perform carboxydo-trophic hydrogenesis (Fig. S17). However, carboxydo-trophic hydrogenesis and Wood–Ljungdahl pathway were not simultaneously found in other reference genomes of genus *Desulfitobacterium* (Table S5), which historically included the majority of *Desulfitobacterium_A*. The presence of *Desulfitobacterium_A* L17 implied that mesophilic carboxydotrophs could encode carboxydotrophic hydro-genesis and Wood–Ljungdahl pathway simultaneously, which has been observed in thermophilic carboxydotroph *Calderihabitans maritimus* [83]. The discovered MAG L4 was *Acetobacterium wieringae* that can grow on CO as sole carbon and energy source [73].

Acetate resulting from Wood–Ljungdahl pathway can be used for propionate production, where incomplete reductive citrate cycle (from acetyl-CoA to succinyl-CoA) and the conversion of succinyl-CoA to propionate are combined. Six MAGs encoding the complete enzymes in propionate production composed group C (Figs. 5 and S15, Dataset S10 and Dataset S11). Three under-characterized MAGs H8, H18, and H20 and a discovered MAG H12 were assigned to genus *Propionicimonas*, of which propionate production could be stimulated with acetate [84]. Only two species of this genus were isolated, *P. paludicola* and *P. ferrireducens*, and some physiological characteristics in this genus showed distinct differences [84, 85]. Additionally, the previous studies on the mixed microbial cultures fed with CO rarely reported the microbes producing propionate. The emergence of *Propionicimonas* spp. in this study not only broadened the genome information of *Propionicimonas*, but also implied the crucial role of *Propionicimonas* in the conversion of CO to propionate, as well as its tolerance to CO. The remaining under-characterized MAG in group C was *Rhodoplanes* H3 that could encode carboxydotrophic hydrogenesis as discussed above, and the other discovered MAG H10 was assigned to genus *Petrimonas* of which some species were also detected in previous studies [34, 69].

Carbon chain elongation

Acetate and propionate can be further elongated into longer carbon chain carboxylates via RBO pathway [86, 87]. The first step of RBO elongates an acyl-CoA by two carbon atoms to form an oxoacyl-CoA, which can be catalyzed by two types of thiolase. Compared with type I thiolase, the substrates of type II thiolase are usually two acetyl-CoA but potentially an acetyl-CoA and a different acyl-CoA. Therefore, type II thiolase mainly participates in butyrate metabolism, and type I thiolase can engage in other longer carbon chain carboxylate production in addition to butyrate production. As per thiolase type, ten MAGs were separated into two groups: group D where the complete enzymes in butyrate production were encoded, and group E that could encode the complete enzymes in synthesizing longer carbon chain carboxylates in addition to butyrate (Figs. 5 and S15, Dataset S10 and Dataset S11, Supplementary Notes).

Group D comprised five under-characterized and five discovered MAGs. The complete genes of Wood–Ljungdahl and RBO pathway existed in the genome of *Desulfito-bacterium_A* L17 in group D. This result suggested that *Desulfitobacterium_A* L17 could perform carboxydotrophic acetogenesis and butyrate production in a single cell, in addition to carboxydotrophic hydrogenesis as discussed above. Carbon chain elongation using syngas fermentation effluent was separated into two sequential reactors [14, 88], which could reduce the inhibition effects of CO on carbon chain elongation microbes and could easily maintain the optimum condition for each stage. *Desulfitobacterium_A* L17 provided a possibility to integrate syngas fermentation and carboxylate elongation using single species, which

could overcome the drawbacks of two-stage reactors; for example, more complicated operation and increased cost [69]. MAG H7 in group D was a novel species of genus *Oscillibacter*, of which the type species is a strictly anaerobic and valerate-producing microbe [89]. An isolate *Oscillibacter* sp. C5 can utilize CO and produce valerate [90]. Additionally, *Oscillibacter* was a dominant genus in a biological CO-converting system [91]. Group E consisted of four discovered and two under-characterized MAGs, of which *Rhodoplanes* H3 and Acetonemaceae H17 might perform CO oxidation. Other bacterial MAGs in this work also had potential in multiple metabolic processes, such as CO oxidation, acetogenesis, and carbon chain elongation (Fig. 5). These MAGs extended the functional redundancy in the conversion of CO to end-products, increasing the overall stability of the CO-driven microbiomes. Further investigations however should be undertaken to explore which pathway will be principally expressed under different CO pressures.

Methane production

Methanogens are the best-studied carboxydotrophic archaea. Two under-characterized and three discovered MAGs were classified as methanogens, constituting group F (Figs. 5 and S15, Dataset S10 and Dataset S11, Supplementary Notes). *Methanobacterium_C* H15, *Methanobacterium_A* L22, and *Methanobacterium formicicum* L9 not only encoded the complete enzymes in hydrogenotrophic methanogenesis, but also harbored the complete genes of CODH/ACS complex (*cdhABCDE*, Fig. S18). Therefore, these three MAGs had potential in carboxydotrophic methanogenesis, which appears to proceed via a common CO_2 reduction pathway [29, 92]. The CODH/ACS complex in methanogens is suggested to mainly participate in assimilatory metabolism [77], and these three MAGs contained the complete genes in the proposed acetogenesis of methanogens. A proteomic analysis of *Methanothermobacter marburgensis* observed higher abundances of CODH/ACS-related proteins and acetate formation in the presence of CO [25]. Furthermore, acetate was a major metabolite of CO-fed *Methanosarcina acetivorans* [21]. Therefore, the Methanobacteriaceae MAGs in group F might also participate in acetate production in addition to methanogenesis. The other archaeal MAGs H22 and L23 were assigned to *Methanothrix soehngenii* and a novel species of *Methanomassiliicoccus*, respectively. Acetoclastic methanogen *M. soehngenii* might contribute to the CH_4 production under low CO pressure since acetoclastic methanogenesis could be dominant when CO pressure was below 0.5 atm [34, 74]. The methanogenic activity of *Methanomassiliicoccus* is limited to methylotrophic methanogenesis with H_2 [93, 94]. The existence of *Methanomassiliicoccus* L23 was somewhat surprising because no methanol or methylamines was detected in this work. The data available for analyzing the function of *Methanomassiliicoccus* L23 are limited, and future works are necessary to explore the role of *Methanomassiliicoccus* in a CO-driven microbiome.

As per the potential functions of the MAGs, the carbon flux and putative microbial interactions were constructed (Fig. 5). CO was first captured by group A, which reduced the inhibition effects of CO and provided available carbon sources for other function guilds. In group B, CO_2 or CO was further converted into acetate, an important chemical and precursor for the synthesis of longer carbon chain carboxylates in groups C, D, and E. In addition to these valuable carboxylates, the primary biofuel was CH_4, which was produced by the methanogens in group F.

Conclusions

The time-series analysis of the isotope-labeled 16S rRNA genes revealed the different dynamic succession of the functional microbiotas under two CO pressures, proposing the essential roles of *Acetobacterium* and *Rhodoplanes* under high CO and low CO pressure, respectively. *Methanobacterium* was the predominant archaeal genus under two CO pressures, suggesting its wide tolerance range to CO. In addition to community structure, this work also shed light on the enriched functional potential of the microbiomes under high CO pressure, presenting greater potential in synthesizing carboxylates and maintaining fundamental metabolism. Genome-centric metagenomics provided genomic insights into the under-characterized taxa, which might play a key role in the conversion of CO to carboxylates or methane. Some under-characterized taxa could encode complete enzymes in multiple pathways; for instance, both under-characterized *Rhodoplanes* sp. and *Desulfitobacterium_A* sp. might perform CO oxidation and carboxylate production. The under-characterized *Rhodoplanes* sp. expanded the phylogenetical diversity of mesophilic hydrogenogenic carboxydotrophs which is far less common. Moreover, the emergence of the under-characterized *Desulfitobacterium_A* sp. implied that Wood–Ljungdahl and RBO pathway could be encoded in a single cell. These versatile taxa could improve the functional redundancy in CO conversion, increasing the stability of the CO-driven microbiomes under variable CO pressure. These reconstructed genomes provided a comprehensive genomic baseline for further CO-converting studies. Based on the metabolic reconstruction of the MAGs, the microbial interactions and food web in the CO-driven microbiomes were established, improving our understanding in mediating the bioproduct synthesis from CO. Further studies are necessary to validate and quantify the contribution of each species to

CO conversion, as well as to investigate which pathway is primarily expressed in versatile species through improved sequencing technology and sensitive metatranscriptome/ metaproteome.

Data availability

All sequencing data have been submitted to NCBI Sequence Read Archive under the project ID PRJNA616065, PRJNA616085, and PRJNA666762. The BioSample number for individual data can be found in Dataset S12.

Compliance with ethical standards

Conflict of interest The authors declare no competing interests.

Publisher's note Springer Nature remains neutral with regard to jurisdictional claims in published maps and institutional affiliations.

References

1. Sokolova TG, Henstra AM, Sipma J, Parshina SN, Stams AJ, Lebedinsky AV. Diversity and ecophysiological features of thermophilic carboxydotrophic anaerobes. FEMS Microbiol Ecol. 2009;68:131–41.

2. King GM, Weber CF. Distribution diversity and ecology of aerobic CO-oxidizing bacteria. Nat Rev Microbiol. 2007;5:107–18.

3. Yoneda Y, Kano SI, Yoshida T, Ikeda E, Fukuyama Y, Omae K, et al. Detection of anaerobic carbon monoxide-oxidizing thermophiles in hydrothermal environments. FEMS Microbiol Ecol. 2015;91:fiv093.

4. Oelgeschläger E, Rother M. Carbon monoxide-dependent energy metabolism in anaerobic bacteria and archaea. Arch Microbiol. 2008;190:257–69.

5. Tiquia-Arashiro SM. Thermophilic carboxydotrophs and their applications in biotechnology. 1st ed. New York, USA: Springer International Publishing; 2014.

6. Esquivel-Elizondo S, Delgado AG, Krajmalnik-Brown R. Evolution of microbial communities growing with carbon monoxide, hydrogen and carbon dioxide. FEMS Microbiol Ecol. 2017;93:fix076.

7. Ferry JG. CO dehydrogenase. Annu Rev Microbiol. 1995;49:305–33.

8. Thauer RK, Jungermann K, Decker K. Energy conservation in chemotrophic anaerobic bacteria. Bacteriol Rev. 1977;41:100–80.

9. Zafiriou OC, Andrews SS, Wang W. Concordant estimates of oceanic carbon monoxide source and sink processes in the Pacific yield a balanced global "blue-water" CO budget. Glob Biogeochem Cycles. 2003;17:15.

10. Islam ZF, Cordero PRF, Feng J, Chen Y-J, Bay SK, Jirapanjawat T, et al. Two Chloroflexi classes independently evolved the ability to persist on atmospheric hydrogen and carbon monoxide. ISME J. 2019;13:1801–13.

11. Cordero PRF, Bayly K, Man Leung P, Huang C, Islam ZF, Schittenhelm RB, et al. Atmospheric carbon monoxide oxidation is a widespread mechanism supporting microbial survival. ISME J. 2019;13:2868–81.

12. King GM. Characteristics and significance of atmospheric carbon monoxide consumption by soils. Chemosphere Glob Change Sci. 1999;1:53–63.

13. Köpke M, Held C, Hujer S, Liesegang H, Wiezer A, Wollherr A, et al. Clostridium ljungdahlii represents a microbial production platform based on syngas. Proc Natl Acad Sci USA. 2010;107:13087–92.

14. Kucek LA, Spirito CM, Angenent LT. High n-caprylate productivities and specificities from dilute ethanol and acetate: chain elongation with microbiomes to upgrade products from syngas fermentation. Energy Environ Sci. 2016;9:3482–94.

15. Lü F, Zhang H, Shao L, He P. Loop bioenergy production and carbon sequestration of polymeric waste by integrating biochemical and thermochemical conversion processes: a conceptual framework and recent advances. Renew Energ. 2018;124:202–11.

16. Fabbri D, Torri C. Linking pyrolysis and anaerobic digestion (Py-AD) for the conversion of lignocellulosic biomass. Curr Opin Biotechnol. 2016;38:167–73.

17. Han W, He P, Shao L, Lü F. Road to full bioconversion of biowaste to biochemicals centering on chain elongation: a mini review. J Environ Sci (China). 2019;86:50–64.

18. Mohammadi M, Najafpour GD, Younesi H, Lahijani P, Uzir MH, Mohamed AR. Bioconversion of synthesis gas to second generation biofuels: a review. Renew Sust Energ Rev. 2011;15:4255–73.

19. Liew F, Martin ME, Tappel RC, Heijstra BD, Mihalcea C, Kopke M. Gas fermentation-A flexible platform for commercial scale production of low-carbon-fuels and chemicals from waste and renewable feedstocks. Front Microbiol. 2016;7:694.

20. Diender M, Uhl PS, Bitter JH, Stams AJ, Sousa DZ. High rate biomethanation of carbon monoxide-rich gases via a thermophilic synthetic coculture. ACS Sustain Chem Eng. 2017;6:2169–76.

21. Rother M, Metcalf WW. Anaerobic growth of Methanosarcina acetivorans C2A on carbon monoxide: an unusual way of life for a methanogenic archaeon. Proc Natl Acad Sci USA. 2004;101: 16929–34.

22. Bertsch J, Müller V. CO metabolism in the acetogen Acetobacterium woodii. Appl Environ Microbiol. 2015;81:5949–56.

23. Henstra AM, Sipma J, Rinzema A, Stams AJ. Microbiology of synthesis gas fermentation for biofuel production. Curr Opin Biotechnol. 2007;18:200–6.

24. Munasinghe PC, Khanal SK. Biomass-derived syngas fermentation into biofuels: opportunities and challenges. Bioresour Technol. 2010;101:5013–22.

25. Diender M, Pereira R, Wessels HJ, Stams AJ, Sousa DZ. Proteomic analysis of the hydrogen and carbon monoxide metabolism of Methanothermobacter marburgensis. Front Microbiol. 2016;7:1049.

26. Luo G, Wang W, Angelidaki I. Anaerobic digestion for simultaneous sewage sludge treatment and CO biomethanation: process performance and microbial ecology. Environ Sci Technol. 2013; 47:10685–93.

27. Brady AL, Sharp CE, Grasby SE, Dunfield PF. Anaerobic carboxydotrophic bacteria in geothermal springs identified using stable isotope probing. Front Microbiol. 2015;6:897.

28. Omae K, Fukuyama Y, Yasuda H, Mise K, Yoshida T, Sako Y. Diversity and distribution of thermophilic hydrogenogenic carboxydotrophs revealed by microbial community analysis in sediments from multiple hydrothermal environments in Japan. Arch Microbiol. 2019;201:969–82.

29. Diender M, Stams AJ, Sousa DZ. Pathways and bioenergetics of anaerobic carbon monoxide fermentation. Front Microbiol. 2015;6:1275.

30. Esquivel-Elizondo S, Maldonado J, Krajmalnik-Brown R. Anaerobic carbon monoxide metabolism by Pleomorphomonas carboxyditropha sp. nov., a new mesophilic hydrogenogenic carboxydotroph. FEMS Microbiol Ecol. 2018;94:fiy056.

31. Esquivel-Elizondo S, Delgado AG, Rittmann BE, Krajmalnik-Brown R. The effects of CO2 and H2 on CO metabolism by pure and mixed microbial cultures. Biotechnol Biofuels. 2017;10:220.

32. Wang HJ, Dai K, Wang YQ, Wang HF, Zhang F, Zeng RJ. Mixed culture fermentation of synthesis gas in the microfiltration and ultrafiltration hollow-fiber membrane biofilm reactors. Bioresour Technol. 2018;267:650–6.

33. Sipma J, Lens PNL, Stams AJM, Lettinga G. Carbon monoxide conversion by anaerobic bioreactor sludges. FEMS Microbiol Ecol. 2003;44:271–7.

34. Navarro SS, Cimpoia R, Bruant G, Guiot SR. Biomethanation of syngas using anaerobic sludge: shift in the catabolic routes with the CO partial pressure increase. Front Microbiol. 2016;7:1188.

35. Quince C, Walker AW, Simpson JT, Loman NJ, Segata N. Shotgun metagenomics, from sampling to analysis. Nat Biotechnol. 2017; 35:833–44.

36. Jameson E, Taubert M, Coyotzi S, Chen Y, Eyice Ö, Schäfer H, et al. DNA-, RNA-, and protein-based stable-isotope probing for high-throughput biomarker analysis of active microorganisms. In: Streit WR, Daniel R, editors. Metagenomics. 2nd ed. New York, NY, USA: Springer International Publishing; 2017. p. 57–74.

37. Coyotzi S, Pratscher J, Murrell JC, Neufeld JD. Targeted metagenomics of active microbial populations with stable-isotope probing. Curr Opin Biotechnol. 2016;41:1–8.

38. Chen Y, Murrell JC. When metagenomics meets stable-isotope probing: progress and perspectives. Trends Microbiol. 2010;18: 157–63.

39. Neufeld JD, Wagner M, Murrell JC. Who eats what, where and when? Isotope-labelling experiments are coming of age. ISME J. 2007;1:103–10.

40. Dumont MG, Murrell JC. Stable isotope probing—linking microbial identity to function. Nat Rev Microbiol. 2005;3:499–504.

41. Schloss PD, Handelsman J. Biotechnological prospects from metagenomics. Curr Opin Biotechnol. 2003;14:303–10.

42. Saidi-mehrabad A, He Z, Tamas I, Sharp CE, Brady AL, Rochman FF, et al. Methanotrophic bacteria in oilsands tailings ponds of northern Alberta. ISME J. 2013;7:908–21.

43. Eyice O, Namura M, Chen Y, Mead A, Samavedam S, Schafer H. SIP metagenomics identifies uncultivated Methylophilaceae as dimethylsulphide degrading bacteria in soil and lake sediment. ISME J. 2015;9:2336–48.

44. Ziels RM, Sousa DZ, Stensel HD, Beck DAC. DNA-SIP based genome-centric metagenomics identifies key long-chain fatty acid-degrading populations in anaerobic digesters with different feeding frequencies. ISME J. 2018;12:112–23.

45. Wilhelm RC, Singh R, Eltis LD, Mohn WW. Bacterial contributions to delignification and lignocellulose degradation in forest soils with metagenomic and quantitative stable isotope probing. ISME J. 2018;13:413–29.

46. Lü F, Guo K, Duan H, Shao L, He PJ. Exploit carbon materials to accelerate initiation and enhance process stability of CO anaerobic open-culture fermentation. ACS Sustain Chem Eng. 2018;6:2787–96.

47. Bates ST, Berg-Lyons D, Caporaso JG, Walters WA, Knight R, Fierer N. Examining the global distribution of dominant archaeal populations in soil. ISME J. 2011;5:908–17.

48. Callahan BJ, McMurdie PJ, Rosen MJ, Han AW, Johnson AJA, Holmes SP. DADA2: high-resolution sample inference from Illumina amplicon data. Nat Methods. 2016;13:581–3.

49. Rognes T, Flouri T, Nichols B, Quince C, Mahé F. VSEARCH: a versatile open source tool for metagenomics. PeerJ. 2016;4:e2584.

50. Bolyen E, Rideout JR, Dillon MR, Bokulich NA, Abnet CC, Al-Ghalith GA, et al. Reproducible, interactive, scalable and extensible microbiome data science using QIIME 2. Nat Biotechnol. 2019;37:852–7.

51. Oksanen J, Blanchet F, Friendly M, Kindt R, Legendre P, McGlinn D, et al. Vegan: community ecology package. 2018. R package version 2.5-3; 2017.

52. Zhou J, Deng Y, Luo F, He Z, Yang Y. Phylogenetic molecular ecological network of soil microbial communities in response to elevated CO2. Mbio. 2011;2:e00122–11.

53. Zhou Y, Chen Y, Chen S, Gu J. fastp: an ultra-fast all-in-one FASTQ preprocessor. Bioinformatics. 2018;34:i884–90.

54. Nurk S, Meleshko D, Korobeynikov A, Pevzner PA. metaSPAdes: a new versatile metagenomic assembler. Genome Res. 2017;27: 824–34.

55. Wu Y-W, Simmons BA, Singer SW. MaxBin 2.0: an automated binning algorithm to recover genomes from multiple metagenomic datasets. Bioinformatics. 2015;32:605–7.

56. Kang DD, Froula J, Egan R, Wang Z. MetaBAT, an efficient tool for accurately reconstructing single genomes from complex microbial communities. PeerJ. 2015;3:e1165.

57. Alneberg J, Bjarnason BS, De Bruijn I, Schirmer M, Quick J, Ijaz UZ, et al. Binning metagenomic contigs by coverage and composition. Nat Methods. 2014;11:1144–6.

58. Parks DH, Imelfort M, Skennerton CT, Hugenholtz P, Tyson GW. CheckM: assessing the quality of microbial genomes recovered from isolates, single cells, and metagenomes. Genome Res. 2015;25:1043–55.

59. Olm MR, Brown CT, Brooks B, Banfield JF. dRep: a tool for fast and accurate genomic comparisons that enables improved genome recovery from metagenomes through de-replication. ISME J. 2017;11:2864–8.

60. Uritskiy GV, DiRuggiero J, Taylor J. MetaWRAP—a flexible pipeline for genome-resolved metagenomic data analysis. Microbiome. 2018;6:158.

61. Chaumeil P-A, Mussig AJ, Hugenholtz P, Parks DH. GTDB-Tk: a toolkit to classify genomes with the genome taxonomy database. Bioinformatics. 2018;36:1925–7.

62. Parks DH, Chuvochina M, Chaumeil P-A, Rinke C, Mussig AJ, Hugenholtz P. A complete domain-to-species taxonomy for bacteria and archaea. Nat Biotechnol. 2020;38:1079–86.

63. Hyatt D, Chen G-L, LoCascio PF, Land ML, Larimer FW, Hauser LJ. Prodigal: prokaryotic gene recognition and translation initiation site identification. BMC Bioinform. 2010;11:119.

64. Huerta-Cepas J, Forslund K, Coelho LP, Szklarczyk D, Jensen LJ, von Mering C, et al. Fast genome-wide functional annotation through orthology assignment by eggNOG-mapper. Mol Biol Evol. 2017;34:2115–22.

65. Franzosa EA, McIver LJ, Rahnavard G, Thompson LR, Schirmer M, Weingart G, et al. Species-level functional profiling of metagenomes and metatranscriptomes. Nat Methods. 2018;15: 962–8.

66. Daniels L, Fuchs G, Thauer RK, Zeikus JG. Carbon monoxide oxidation by methanogenic bacteria. J Bacteriol. 1977;132:118–26.

67. Guiot SR, Cimpoia R, Carayon G. Potential of wastewater-treating anaerobic granules for biomethanation of synthesis gas. Environ Sci Technol. 2011;45:2006–12.

68. Alves JI, Stams AJ, Plugge CM, Alves MM, Sousa DZ. Enrichment of anaerobic syngas-converting bacteria from thermophilic bioreactor sludge. FEMS Microbiol Ecol. 2013;86:590–7.

69. He P, Han W, Shao L, Lü F. One-step production of C6–C8 carboxylates by mixed culture solely grown on CO. Biotechnol Biofuels. 2018;11:4.

70. García-García N, Tamames J, Linz AM, Pedrós-Alió C, Puente-Sánchez F. Microdiversity ensures the maintenance of functional

microbial communities under changing environmental conditions. ISME J. 2019;13:2969–83.

71. Kleindienst S, Grim S, Sogin M, Bracco A, Crespo-Medina M, Joye SB. Diverse, rare microbial taxa responded to the deepwater horizon deep-sea hydrocarbon plume. ISME J. 2016;10:400–15.

72. Kashtan N, Roggensack SE, Berta-Thompson JW, Grinberg M, Stepanauskas R, Chisholm SW. Fundamental differences in diversity and genomic population structure between Atlantic and Pacific Prochlorococcus. ISME J. 2017;11:1997–2011.

73. Arantes AL, Moreira JP, Diender M, Parshina SN, Stams AJ, Alves MM, et al. Enrichment of anaerobic syngas-converting communities and isolation of a novel carboxydotrophic acetobacterium wieringae strain JM. Front Microbiol. 2020;11:58.

74. Grimalt-Alemany A, Łężyk M, Kennes-Veiga DM, Skiadas IV, Gavala HN. Enrichment of mesophilic and thermophilic mixed microbial consortia for syngas biomethanation: the role of kinetic and thermodynamic competition. Waste Biomass Valoriz. 2020;11:465–81.

75. Carr SA, Jungbluth SP, Eloe-Fadrosh EA, Stepanauskas R, Woyke T, Rappé MS, et al. Carboxydotrophy potential of uncultivated Hydrothermarchaeota from the subseafloor crustal biosphere. ISME J. 2019;13:1457–68.

76. Fukuyama Y, Inoue M, Omae K, Yoshida T, Sako Y. Chapter three—anaerobic and hydrogenogenic carbon monoxide-oxidizing prokaryotes: versatile microbial conversion of a toxic gas into an available energy. In: Gadd GM, Sariaslani S, editors. Advances in applied microbiology. 1st ed. Cambridge, MA, USA: Academic Press; 2020. p. 99–148.

77. Techtmann S, Lebedinsky AV, Colman AS, Sokolova TG, Woyke T, Goodwin L, et al. Evidence for horizontal gene transfer of anaerobic carbon monoxide dehydrogenases. Front Microbiol. 2012;3:132.

78. Kerby RL, Ludden PW, Roberts GP. Carbon monoxide-dependent growth of Rhodospirillum rubrum. J Bacteriol. 1995;177:2241–4.

79. Fox JD, He Y, Shelver D, Roberts GP, Ludden PW. Characterization of the region encoding the CO-induced hydrogenase of Rhodospirillum rubrum. J Bacteriol. 1996;178:6200–8.

80. Hussain A, Bruant G, Mehta P, Raghavan V, Tartakovsky B, Guiot SR. Population analysis of mesophilic microbial fuel cells fed with carbon monoxide. Appl Biochem Biotechnol. 2014;172:713–26.

81. Mosbaek F, Kjeldal H, Mulat DG, Albertsen M, Ward AJ, Feilberg A, et al. Identification of syntrophic acetate-oxidizing bacteria in anaerobic digesters by combined protein-based stable isotope probing and metagenomics. ISME J. 2016;10:2405–18.

82. Can M, Armstrong FA, Ragsdale SW. Structure, function, and mechanism of the nickel metalloenzymes, CO dehydrogenase, and acetyl-CoA synthase. Chem Rev. 2014;114:4149–74.

83. Yoneda Y, Yoshida T, Yasuda H, Imada C, Sako Y. A thermophilic, hydrogenogenic and carboxydotrophic bacterium, Calderihabitans maritimus gen. nov., sp. nov., from a marine sediment core of an undersea caldera. Int J Syst Evol Microbiol. 2013;63:3602–8.

84. Akasaka H, Ueki A, Hanada S, Kamagata Y, Ueki K. Propionicimonas paludicola gen. nov., sp. nov., a novel facultatively anaerobic, Gram-positive, propionate-producing bacterium isolated from plant residue in irrigated rice-field soil. Int J Syst Evol Microbiol. 2003;53:1991–8.

85. Zhou G-W, Yang X-R, Wadaan MAM, Hozzein WN, Zheng B-X, Su J-Q, et al. Propionicimonas ferrireducens sp. nov., isolated from dissimilatory iron(III)-reducing microbial enrichment obtained from paddy soil. Int J Syst Evol Microbiol. 2018;68: 1914–8.

86. Angenent LT, Richter H, Buckel W, Spirito CM, Steinbusch KJ, Plugge CM, et al. Chain elongation with reactor microbiomes: open-culture biotechnology to produce biochemicals. Environ Sci Technol. 2016;50:2796–810.

87. Dellomonaco C, Clomburg JM, Miller EN, Gonzalez R. Engineered reversal of the β-oxidation cycle for the synthesis of fuels and chemicals. Nature. 2011;476:355–9.

88. Gildemyn S, Molitor B, Usack JG, Nguyen M, Rabaey K, Angenent LT. Upgrading syngas fermentation effluent using Clostridium kluyveri in a continuous fermentation. Biotechnol Biofuels. 2017;10:83.

89. Iino T, Mori K, Tanaka K, Suzuki K-I, Harayama S. Oscillibacter valericigenes gen. nov., sp. nov., a valerate-producing anaerobic bacterium isolated from the alimentary canal of a Japanese corbicula clam. Int J Syst Evol Microbiol. 2007;57:1840–5.

90. Park S, Yasin M, Kim D, Roh H, Choi I-G, Chang IS. Characterization of CO-utilizing and isovalerate producing acetogen; Oscillibacter sp. C5 isolated from cow feces. KSBB Spring Meeting. 2013:264.

91. Im CH, Kim C, Song YE, Oh S-E, Jeon B-H, Kim JR. Electrochemically enhanced microbial CO conversion to volatile fatty acids using neutral red as an electron mediator. Chemosphere. 2018;191:166–73.

92. O'Brien JM, Wolkin RH, Moench TT, Morgan JB, Zeikus JG. Association of hydrogen metabolism with unitrophic or mixotrophic growth of Methanosarcina barkeri on carbon monoxide. J Bacteriol. 1984;158:373–5.

93. Dridi B, Fardeau M-L, Ollivier B, Raoult D, Drancourt M. Methanomassiliicoccus luminyensis gen. nov., sp. nov., a methanogenic archaeon isolated from human faeces. Int J Syst Evol Microbiol. 2012;62:1902–7.

94. Lang K, Schuldes J, Klingl A, Poehlein A, Daniel R, Brune A. New mode of energy metabolism in the seventh order of methanogens as revealed by comparative genome analysis of "Candidatus Methanoplasma termitum". Appl Environ Microbiol. 2015;81:1338–52.